Nonlin. Processes Geophys., 15, 397–407, 2008
www.nonlin-processes-geophys.net/15/397/2008/

Nonlinear Processes in Geophysics

Spatial relationship between δ^{15}N and elevation in agricultural landscapes

A. Biswas, B. C. Si, and F. L. Walley

Department of Soil Science, University of Saskatchewan, Saskatoon, SK, Canada

Received: 28 September 2007 – Revised: 4 April 2008 – Accepted: 4 April 2008 – Published: 13 May 2008

Abstract. Understanding of the nitrogen (N) cycle and its spatial variability is important for managing ecosystems. Soil δ^{15}N, as an important indicator of different soil nitrogen cycling processes, may provide critical information about the spatial variability in soil N cycling. The objective of this study was to examine the dominant landscape scale variability of δ^{15}N, the location of the variability and its spatial relationship with elevation. Soil δ^{15}N and elevation were measured along two transects (Davidson and Elstow, Saskatchewan, Canada). Each transect had 128 points with 3 m sampling intervals. Higher δ^{15}N values typically occurred in topographic depressions as compared to knolls. The coefficient of determination revealed a significant linear relationship between δ^{15}N and elevation (r^2=0.27) at Davidson whereas no relationship (r^2=0.00) was detected for the Elstow transect. However, wavelet spectra, cross wavelet, and squared wavelet coherency analysis revealed spatial relationships between δ^{15}N and elevation at both sites. A strong coherency between δ^{15}N and elevation at large scales (96 m or more) was detected for both transects. The Davidson transect showed an out of phase coherency at a topographically elevated area at the beginning and the end of the transect. The Elstow transect had a strong out of phase correlation (negative relationship) at the middle of the transect (corresponding to a depressions) indicating a location dependent relationship between δ^{15}N and elevation. The relationship between δ^{15}N and elevation reflects the effects of hydrology and soil water content over the landscape on N cycling processes.

1 Introduction

In agricultural systems, organic N typically dominates the total soil N pool and an estimated 1 to 3% of soil organic N mineralizes and enters the inorganic N pool annually (Keeney, 1982), mainly from labile fractions (Jenkinson and Parry, 1989). Variations in the nature and magnitude of N-cycling processes within a landscape ultimately control the availability of mineral N (NH_4^+ and NO_3^-) which is essential for agricultural production and likewise is the source of serious environmental pollution (e.g., NO_3^- contamination of groundwater and emissions of N_2O, an important greenhouse gas). Thus, there is a keen interest in understanding patterns of soil N availability and N-cycling processes within landscapes.

Although complex, soil N dynamics can be revealed in the natural abundances of ^{15}N, a relatively rare and stable isotope of N (Bedard-Haughn et al., 2003). The detection of small differences in the ratio between ^{15}N and ^{14}N, usually expressed in per mil deviations from atmospheric N (i.e., δ^{15}N) has been used widely as an integrator of the N cycle (Robinson, 2001). Variations in δ^{15}N relative to atmospheric N occur as a result of isotopic fractionation in physical, chemical and biological processes in which reactions are incomplete and typically favour the lighter ^{14}N isotope (Höberg, 1997; Kendall, 1998). As a consequence, various soil N pools develop distinctly different δ^{15}N signals. Moreover, the δ^{15}N of the total soil N is dominated by the isotopic signature of the relatively recalcitrant soil N fraction which, according to Johannisson and Höberg (1994), is stable over decades.

Although each step of a biologically mediated reaction has its own impact on the dgree of isotopic fractionation, the overall observed isotopic fractionation effect (β_{obs}) can be calculated according to Shearer and Kohl (1986):

$$\beta_{obs} = (^{15}N/^{14}N)_{substrate}/\ (^{15}N/^{14}N)_{product}$$

In soil, biological N transformations that contribute most strongly to isotopic fractionation include nitrification, denitrification and ammonia volatilization. Nitrification, a biologically mediated process in which ammonium (NH_4^+) is oxidized to nitrate (NO_3^-) as the final product has an estimated β_{obs} of 1.012–1.029 (Shearer and Kohl, 1986). Microbially mediated denitrification is the reduction of NO_3^- or NO_2^- to N_2O or N_2 and fractionation during this

Correspondence to: B. Si
(bing.si@usask.ca)

process reportedly is highly variable (Höberg, 1997) with fractionation factors ranging from 1.000 to 1.033 (Mariotti et al., 1981; Bryan et al., 1983; Yoshida et al., 1989; Korom, 1992). The denitrified product (N_2O and N_2) is generally ^{15}N depleted because $^{15}NO_3^-$ reacts more slowly than $^{14}NO_3^-$ leaving the ^{15}N enriched unreacted NO_3^- in the environment (Sutherland et al., 1993). Ammonia volatilization is the mass transfer of N from the soil system as ammonia gas and involves several steps during which fractionation can occur such that the net fractionation can be large (e.g., 1.029) (Höberg, 1997). Consequently, where volatilization of ammonia is a significant process, (e.g., in calcareous soils), the soil N remaining becomes enriched with ^{15}N.

Given the dynamic nature of the different soil N cycling processes, it is unsurprising that δ^{15}N in soil is reportedly highly variable, ranging from 1 to 16 (Cheng et al., 1964), -7 to 18 (Bremner and Tabatabai, 1973), a mean value 3.03 (Riga et al., 1970), 9.22 (Shearer et al., 1978) or a value >10 (Townsend, 2001). Various authors have attempted to explain in situ variability within a broad geographic area. For example, Riga et al. (1970) showed the relationship between δ^{15}N and plant cover or soil management practices whereas Kreitler (1975), Heaton (1986) and Herbel and Spalding (1993) explained variations in δ^{15}N based on the sources of N. Because biological processes contribute to the δ^{15}N signature in soils, factors controlling these processes, such as topography (Karamanos et al., 1981; Selles et al., 1986; Venterea et al., 2003), hydrology (Elliott and de Jong, 1992), C availability (Smith and Tiedje, 1979), substrate availability (e.g., NO_3^- and NO_2^-), pH (Blackmer and Bremner, 1978), redox potential (Sorenson et al., 1980), and microbial communities and population, presumably are related to the ultimate δ^{15}N signature of the soil.

Topography largely controls site hydrology (Zebarth and de Jong, 1989; Pennock et al., 1994; Moulin et al., 1994) and consequently the microbially mediated soil N transformation processes, ultimately contributing to a spatial variation in δ^{15}N content (Karamanos et al., 1981; Selles et al., 1986; Sutherland et al., 1991; Bedard-Haughn et al., 2003). A few studies examined δ^{15}N variability in soil using conventional statistics (Cheng et al., 1964; Broadbent et al., 1980; Karamanos et al., 1981; and Shearer and Kohl, 1986). Karamanos et al. (1981) and Selles et al. (1986) found higher δ^{15}N values in lower topographic positions than on knolls. Using geostatistics, Sutherland et al. (1993) found elevation to be the most important topographic factor controlling the variability of δ^{15}N in soil and crops. These statistical techniques can explain the variation over space, but they cannot describe the scale at which this variation is at a maximum or minimum (Lemke et al., 1998; Si and Farrell, 2004).

The information about the dominant scale and location of variations is important in understanding the dominant processes in agricultural fields. Spectral analysis can be used to identify the dominant scale of variation, but the spatial (or location) information cannot be retained. In addition, geostatistical and spectral analyses are only applicable to stationary fields, where different segments of a transect in the fields have identical means and variances. In natural landscapes, δ^{15}N and other soil properties may exhibit spatial trends and are non-stationary. Wavelet analysis, an advanced statistical method, is promising in this type of situation (Mallat, 1999) and can be used to reveal the dominant processes and their location and scale of occurrence over landscapes. Wavelet analysis has been applied to a wide variety of fields, such as geophysics (Kumar and Foufoula-Goergiou, 1997), hydrology (Labat et al., 2000) and soil science (Lark and Webster, 1999, 2001; Si, 2003).

A wavelet is a mathematical function representing a finite small wave form (Graps, 1995) unlike the function used in Fourier analysis, which stretches infinitely. Wavelet analysis divides a spatial series into different frequency components and studies each component using a fully scalable window (wavelet). It calculates the variation in spectrum for every position by shifting the standard function (mother wavelet) along the spatial series. Contraction and dilation of this function, which changes the size of the interval in time and space in the data series, provides information about scale. Si (2003) and Si and Farrell (2004) used wavelet to analyse the scale of soil properties. Unlike Fourier transform, wavelet transform decomposes the variance of a process into a series of coefficients representing the distribution of variance across scale as well as locations (Yates et al., 2006). The wavelet coefficient at each point of the data series and at each scale is obtained (Yates et al., 2006). There are two types of wavelet transforms; continuous and discrete (Si and Zeleke, 2005). Continuous wavelet transform (CWT), which overlaps between wavelet coefficients resulting in redundant information between scale and locations (Yates et al., 2006), is useful for scale analysis of soil properties (Mallat, 1999; Neilsen and Wendorth, 2003; Si, 2003; He et al., 2007). The discrete wavelet transform (DWT) has certain advantages over continuous wavelet transform in some aspects. The CWT is simpler to implement and easy to interpret whereas DWT is fast to compute. However, it is easy to explain the local relationship between variables using CWT (Torrence and Compo, 1998; Grinsted et al., 2004; Si and Zeleke, 2005). Wavelet analysis gives the variations in variables, whereas the cross wavelet analysis gives the covariances between them (Si and Zeleke, 2005). Cross wavelet analysis is an important tool for identifying the correlation between variables. Cross wavelet spectra, or the covariance at a scale, are the product of the two variables at that scale. It is sometimes difficult to understand the relationship from covariances or cross wavelet spectra, because the high covariance at the scale and location may simply be due to the high wavelet spectrum for one variable (not both), which may not suggest high correlation (Si and Zeleke, 2005). Wavelet coherency can further elucidate relationships in that case.

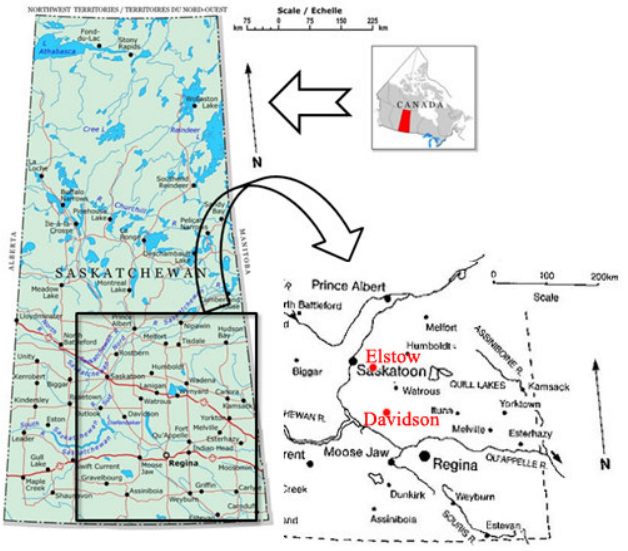

Fig. 1. Physical location of the two sampling sites; Davidson and Elstow (Natural Resources Canada, 2001).

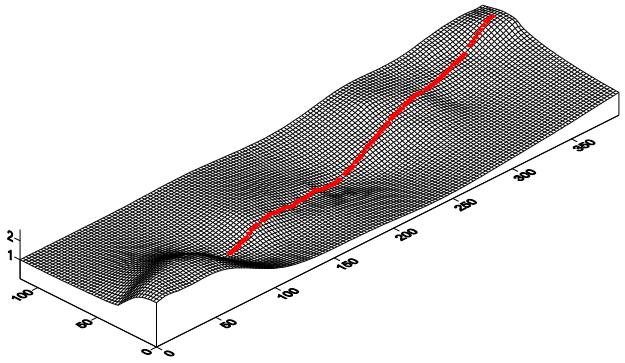

Fig. 2. Physiographic view of the Davidson transect area.

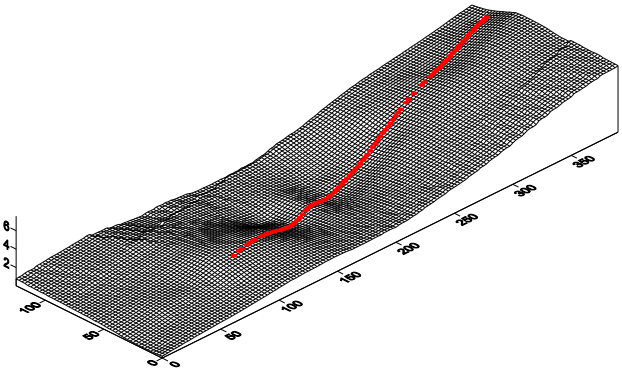

Fig. 3. Physiographic view of the Elstow transect area.

There is little information available about the scale dependent relationship between δ^{15}N in soil and elevation, particularly in agricultural fields. However in order to evaluate the dominant landscape scale and location controlling δ^{15}N variation, it is important to further explore this relationship. The objective of this study was to elucidate the dominant landscape scale and location of δ^{15}N variation by examining the spatial relationship between δ^{15}N and elevation. In this study, we used wavelet spectral analysis, cross wavelet, and wavelet coherency as tools to describe the relationship between δ^{15}N and elevation over two transects as N-cycling processes may be contributing to the relationship.

2 Materials and methods

2.1 Study site

Sampling transects, 384 m in length and extending over a range of landscape positions (i.e., from knolls to depressions), were established at sites located near Davidson (NE 5-27-28 W2) and Elstow (SW 20-35-28 W2), Saskatchewan, Canada (Fig. 1). Both sites had been under cultivation for more than 50 years, had received regular applications of inorganic fertilizer N during this time period, and had grown a wide range of annual crops including cereals, oilseeds and pulses. Sites were surveyed using a Model Set 5 Sokkisha total station laser theodolite and digital elevation maps were created (Figs. 2 and 3). Soils were sampled in the early spring to a depth of 15 cm at 3 m intervals along the transects. At Elstow, soils are classified mainly as Chernozemic and belong to both the Elstow and Weyburn associations. Soil textures range from silty loam to loam. Slopes at the site are undulating with crossed pattern, and range from 2 to 5%. Soils at Davidson similarly are mainly Chernozemic and belong dominantly to the Elstow association. These are largely calcareous lacustrine deposits underlain by glacial till. Soil texture ranges from silty clay loam to clay loam. Slopes are relatively gentle (gently to gently undulating), ranging from 0.5 to 5%.

2.2 Laboratory analysis

Soils were air-dried, ground and ball-milled prior to analyses. The δ^{15}N was determined according to the procedure described by Bremer and van Kessel (1990) using a dual inlet, dual collector VG micromass 602E (Isotech, Middlewich, England) mass spectrometer. The δ^{15}N of a soil sample is defined as the ratio of nitrogen-15 (^{15}N) to nitrogen-14 (^{14}N) in the sample divided by the ratio observed in standard, atmospheric nitrogen (air):

$$\delta^{15}N(‰) = \left[\frac{\left({}^{15}N/{}^{14}N\right)_{\text{sample}} - \left({}^{15}N/{}^{14}N\right)_{\text{standard}}}{\left({}^{15}N/{}^{14}N\right)_{\text{standard}}} \right] 1000$$

The units of δ^{15}N are given in ‰ (per mil) and the atmospheric N_2 is the standard amount (0.3663 atom % ^{15}N, equivalent to a δ^{15}N value of 0). The enrichment or depletion of δ^{15}N in sample was indicated by plus (+) or minus (−) sign respectively.

2.3 Data analysis

2.3.1 Wavelet analysis

The detailed description of wavelet analysis is given by different authors (Farge, 1992; Kumar and Foufoula-Georgiou 1993, 1997; Torrence and Compo, 1998). We only present the basics regarding wavelet analysis in this paper. A standard mathematical function or "mother wavelet" is used for rescaling and there are a number of 'mother wavelets' for example; Harr, Mexican hat, Meyer, and Morlet wavelets. Mathematically the two basic properties of a wavelet can be expressed as:

$$\int_{-\infty}^{\infty} \psi(x)dx = 0$$

and the square of $\psi(x)$ integrates to unity:

$$\int_{-\infty}^{\infty} \psi^2(x)dx = 1$$

Morlet wavelet can be represented as (Grinsted et al., 2004):

$$\psi(\eta) = \pi^{-1/4} e^{i\varpi\eta - 0.5\eta^2}$$

where, ω is dimensionless frequency and η is dimensionless space. The Morlet wavelet (ω=6) is good for feature extraction because it provides a good balance between space and frequency localization. η=s/x, if the wavelet is stretched in space (x) by varying its scale (s) (Si and Zeleke, 2005). The Fourier period is almost equal to the scale ($\lambda = \frac{4\pi s}{\omega+\sqrt{\omega^2+2}} \approx 1.03s$; Meyer et al., 1993) for the Morlet wavelet (Si and Zeleke, 2005). The continuous wavelet transform for a spatial series of length N (Y_i, i=1, 2, •••, N) with equal incremental distance δx, can be defined as the convolution of Y_i with the scaled and normalized wavelet (Yates et al., 2006), which is implemented using the fast Fourier transform (Torrence and Compo, 1998).

$$W_i^Y(s) = \sqrt{\frac{\delta x}{s}} \sum_{j=1}^{N} Y_j \psi \left[(j-i)\frac{\delta x}{s} \right]$$

Wavelet coefficients, $W_i^Y(s)$, are expressed as a+ib where a and b are the real and imaginary components of $W_i^Y(s)$. For the polar form of complex numbers, $W_i^Y(s) = \left|W_i^Y(s)\right| (\cos\theta + i\sin\theta)$, where $\theta = arc\tan\frac{b}{a}$, which is called the phase or argument of $W_i^Y(s)$ (Si and Zeleke, 2005). The wavelet power spectrum is defined as $\left|W_i^Y(s)\right|^2$ and the local phase can be defined from $W_i^Y(s)$.

2.3.2 Cross Wavelet transform

The cross wavelet power spectrum can be defined as: $\left|W_i^{XY}(s)\right| = \left|W_i^Y(s)\overline{W_i^X(s)}\right|$

where, W_i^X and W_i^Y are the wavelet transforms of the spatial series X and Y. $\overline{W_i^X}$ is the complex conjugate of W_i^X. The complex argument of W_i^{XY} can be interpreted as the local relative phase between X_i and Y_i in the spatial frequency domain (Si and Zeleke, 2005).

2.3.3 Wavelet Squared Coherency

The wavelet coherence of the two spatial series can be defined as (Torrence and Webster, 1999 and Grinsted et al., 2004)

$$R_i^2(s) = \frac{\left|S\left(s^{-1}W_i^{XY}(s)\right)\right|^2}{S\left(s^{-1}\left|W_i^X(s)\right|^2\right) S\left(s^{-1}\left|W_i^Y(s)\right|^2\right)}$$

where, S is a smoothing operator and can be written as

$$S(W) = S_{\text{scale}}\left(S_{\text{space}}(W(s,\tau))\right)$$

where, τ denotes the location and S_{scale} and S_{space} denote the smoothing along the wavelet scale axis and the spatial domain respectively. The normalised real Morlet wavelet (the smoothing function) has a footprint like the Morlet wavelet. Therefore the smoothing along locations can be written as

$$S_{\text{space}}(W(s,\tau))$$

$$= \sum_{k=1}^{N} \left(W(s,\tau)\frac{1}{s\sqrt{2\pi}} \exp\left(-\frac{(\tau - x_k)^2}{2s^2}\right)\right)\Big|_s$$

where, $\frac{1}{s\sqrt{2\pi}}\exp\left(-\frac{\tau^2}{2s^2}\right)$ is a smoothing function. The Fourier transform of this equation is $\exp(-2s^2\omega^2)$ where ω is the frequency (Si and Zeleke, 2005). This equation can be implemented according to the convolution theorem using Fast Fourier transform (FFT) and inverse FFT (IFFT) as

$$S_{\text{space}}\{W(s,\tau)\} = \text{IFFT}\left[\text{FFT}\{W(s,\tau)\}\left\{\exp(-2s^2\omega^2)\right\}\right]$$

The smoothing along the scales can be written as

$$S_{\text{scale}}(Y) = \frac{1}{2m+1}\sum_{j=k-m}^{k+m}\left\{Y\Pi\left(0.6s_j\right)\right\}\Big|_x$$

where, Y is the unknown variable, Π is the rectangle function, $|_x$ means at a fixed x value, m is the number at each side for averaging and j is the index for the scales. The scale decorrelation length of the Morlet wavelet is the factor of 0.6 (Torrence and Compo, 1998).

2.4 Test of statistical significance

The significance test for the local wavelet spectrum, cross wavelet spectrum, and squared wavelet coherency can be done against Gaussian white and red noises (Pardo-Iguzquiza and Rodriguez-Tovar, 2000). White noise data series is not auto correlated as white noise is independently and identically distributed spatial series. In red noises the data values are similar at points separated by one sampling interval and dissimilar at points separated further. Red noise is generally modeled as a univariate lag 1 auto regressive (AR1) process (Torrence and Compo, 1998; Si and Farrell, 2004). The red noise-like behaviour of soil property is very common (Torrence and Compo, 1998; Neilson and Wendorth, 2003; Grinsted et al., 2004; Si and Farrell, 2004). Therefore, we used red noise as the null hypothesis of a statistical test (Si and Zeleke, 2005). In this study, we calculated lag-1 autocorrelation (r) of elevation and δ^{15}N for both transects. For a given r, we generated 1000 realizations of spatial series that have the same mean, variance, and lag-1 autocorrelation coefficient. For each realization we took the wavelet transform and computed the wavelet power, resulting in 1000 values of wavelet power at each scale and location. Because the probability distribution of wavelet power at a scale should be the same at different locations for a large number of realizations, we may pick a location to derive the probability distribution of the wavelet power. Because the centre of the transect has the least edge effect, we took a slice of the local wavelet power (including all scales) from the centre of the transect for each of the 1000 realizations. The value of wavelet power at a scale from the 1000 slices (one from each of the 1000 realizations), were sorted in ascending order. The 900th value (out of 1000) at a scale gives the 90% confidence level or the 10% significance level for that scale (Si and Zeleke, 2005). Wavelet power at different scales may have different values for the 90% confidence level. Wavelet power at a certain scale and location is significantly different from background red noise if the value of the wavelet power is larger than the 90% confidence level or 10% of significance level at that scale. Because there are many values of wavelet power to be tested simultaneously, multiple testing is needed to control the Type I error (Si, 2007). In this study, our approach is very conservative in that a feature is considered as significant at the significance level α only if the feature covers more than α% of the total area of local wavelet spectra (Maraun and Kurths, 2004; Si and Zeleke, 2005). The statistical significance tests for cross wavelet spectrum and coherency were done the same way as the wavelet power.

3 Results and discussion

At Davidson, δ^{15}N had an average of 7.73, a variance of 0.87, a maximum of 9.44 and a minimum of 4.59 (Fig. 4). The median value (7.90) was very similar to the average, suggesting a symmetrical probability distribution. The δ^{15}N values at the two ends of the transect were smaller than the average in the middle of the transect. As the elevation decreased from the origin of the transect, the δ^{15}N showed a considerable increase with the first highest value (8.53) at 69 m from the origin of transect. This sampling point is located in a depression. With the increase in elevation, δ^{15}N decreased to a minimum at location 96 m. Thereafter several small maxima were found between positions 120 m to 210 m. This section corresponded with low elevation. The δ^{15}N again increased (at 285 m in transect) with the decrease in elevation after a small decrease at the transect position of 255 m. The δ^{15}N value showed a negative correlation with the elevation (r^2=0.27).

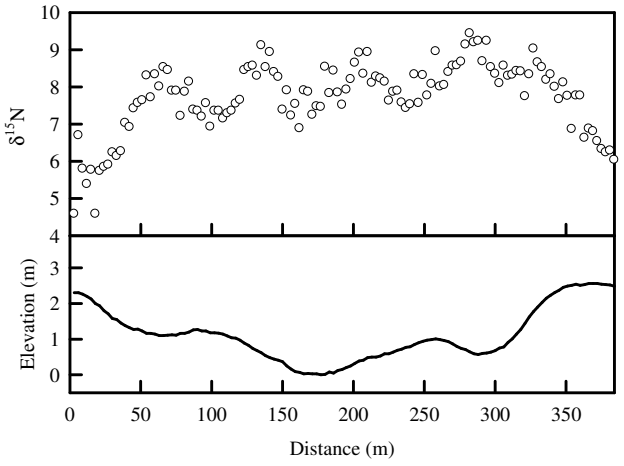

Fig. 4. Diagram of elevation and δ^{15}N of the Davidson transect. The horizontal axis is the distance between the sampling locations and the origin of transect.

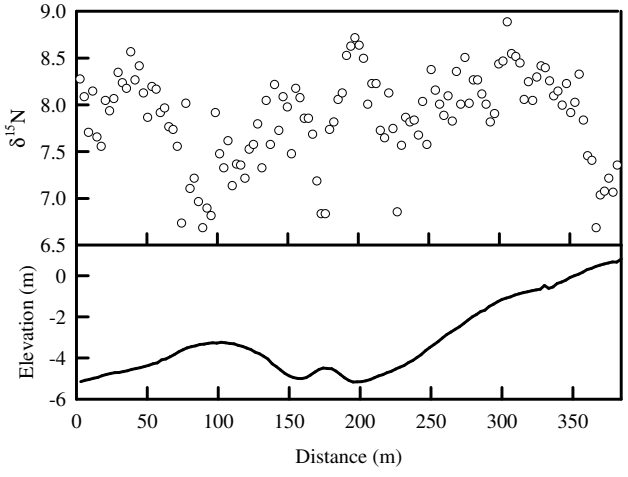

Fig. 5. Diagram of elevation and δ^{15}N of the Elstow transect. The horizontal axis is the distance between the sampling locations and the origin of the transect.

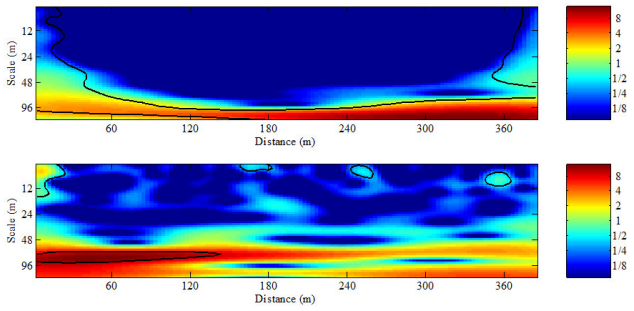

Fig. 6. Local wavelet spectrum of the elevation (top) and δ^{15}N (bottom) value of the Davidson transect. The horizontal axis is the distance between a sampling locations and the origin of the transect. Black solid line indicates the 90 per cent confidence level.

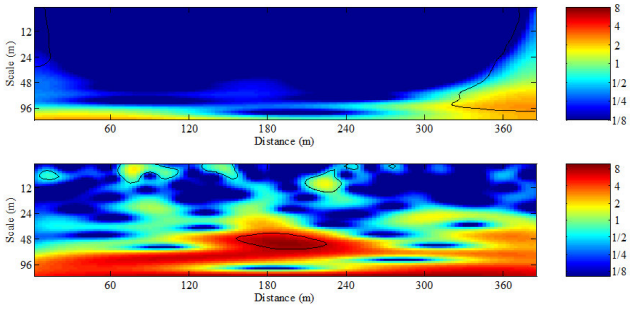

Fig. 7. Local wavelet spectrum of the elevation (top) and δ^{15}N (bottom) value of Elstow transect. The horizontal axis is the distance between a sampling locations and the origin of the transect. Black solid line indicates the 90 per cent confidence level.

At the Elstow transect, the measured δ^{15}N values had a mean of 7.86 and a variance of 0.23 (Fig. 5). Similar to the Davidson transect, the median value (7.92) also was similar to the average (7.86) at the Elstow transect, indicating a symmetrical distribution of δ^{15}N values. The δ^{15}N maxima were located at depressions in the transect, as has been reported by others (Karamanos et al., 1981; Selles et al., 1986) although points not associated with depression sections along the transect shared similar values. An increment of the δ^{15}N value was found at the beginning of the transect, forming a peak. The next two peaks were found at 150 m and 200 m, the two consecutive depression sections. Thereafter, with the continuous increase of the elevation, the δ^{15}N value decreased with the low value at the end of the transect. The correlation coefficient between δ^{15}N and elevation is very low (r^2=0.00).

Figure 6 shows the local wavelet spectrum of the elevation and δ^{15}N in soil of the Davidson transect. The wavelet spectrum of the elevation is quite different from the wavelet spectrum of the δ^{15}N. There is a medium variance (light blue) at small scales at the beginning of the transect. The variance increases (light blue to yellow and red) with the increase in scale at the beginning of the transect. There is a large variance from the beginning of the transect to a distance of 180 m at a large scale (90 m or more). This variance starts from a smaller scale and increases with the increase in scale. There is a medium variance (light blue), which also increases gradually with the scale up to 48 m at the end of the transect. There is a large variance (red and yellow) across the whole transect at the scale of 96 m or more at the beginning of transect and 75 m or more at the end of the transect. These variations are statistically significant, as indicated by the thick contour line (Fig. 6). The area of each significant variation is less than 10 per cent of the total area. These variations are mainly concentrated at the beginning and the end of the transect, corresponding to relatively high elevations. There are some moderate variances (light blue) throughout the transect. This variation increases with the scale as the transect length increases.

The wavelet spectrum for the δ^{15}N values reveals a small scale (<12 m) variation at the locations of 0 m to 18 m, 171 to 177 m, 248 to 254 m, and 350 to 360 m of the transect. These sections are statistically significant. There is a large variation (red) at the scale of 75 m to 90 m over the distance of 15 m to 105 m. A large variation (yellow and red) exists at the scale of 60 m or more over almost the entire transect, except at the section of 132 to 231 m at the scale of 96 to 110 m and 270 to 345 m area at the scale of 90 to 96 m. A number of medium variations (light blue) exist over the transect for almost every scale. A number of peaks in the δ^{15}N values may correspond to these variations. Although each thick black contoured area is statistically significant, the variation is less than 10 per cent of the total area; which means the variation at that scale is less than 10% of the total variation and therefore, it is not possible statistically to rule out these variations from the background red noise.

Figure 7 shows the local wavelet spectrum of the elevation and the δ^{15}N values of the Elstow transect. There is a little variation (0–24 m) at the beginning of the transect. There is also some small to large variation (light blue to yellow) at the end of the transect. These variations start at the small scale, extend up to the scale of 96 m, and increase with the scale. There is large variation (yellow) at the scale of 96 m or more over almost the entire transect, except at the section of 150 m to 270 m of the transect where it shows medium variation (light blue). Medium variations also exist at the scale of 45 m to 96 m at the section of 150 m to 210 m of the transect and at the scale of around 90 m over most of the transect. The thick black contoured line area is statistically significant, but the variation is less than 10 per cent of the total area.

The wavelet spectrum for the δ^{15}N value shows some variations at small scales (Fig. 7). There is quite a large variation (yellow) at the section of 66 to 108 m, 126 to 150 m and 210 to 237 m of transect at the scale of around 24 m. A large variation (red) appears at almost the middle of the transect at the scale of around 48 m which is statistically significant, but this variation is less than the 10 per cent of the total area. A large variation is present at the scale of 45 to 90 m at the section of

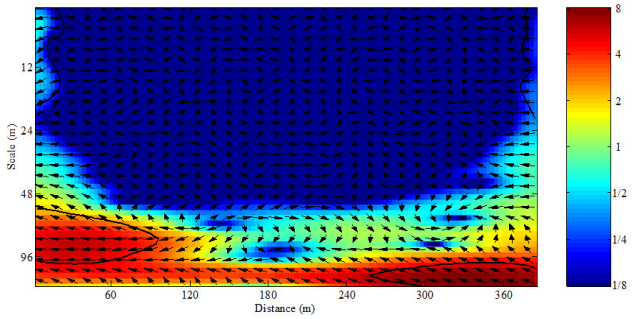

Fig. 8. Local cross wavelet spectra between the elevation and δ^{15}N of the Davidson transect. The horizontal axis shows the distance between sampling locations and the origin of transect. The vertical axis shows the scale. Arrows indicate the phase angles on wavelet spectra. Black solid line indicates the 90 per cent confidence level.

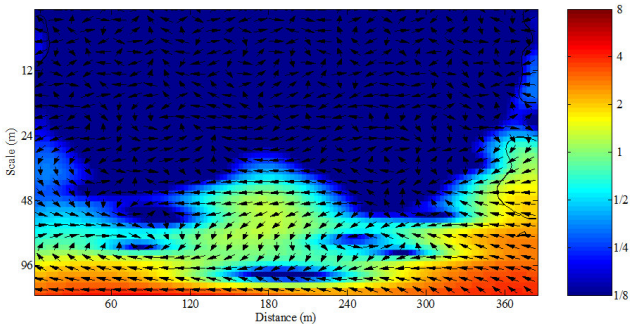

Fig. 9. Local cross wavelet spectra between the elevation and δ^{15}N of the Elstow transect. The horizontal axis shows the distance between sampling locations and the origin of transect. The vertical axis shows the scale. Arrows indicate the phase angles on wavelet spectra. Black solid line indicates the 90 per cent confidence level.

120 to 270 m of the transect. The large variation persists at the scale of 90 m or more over almost the entire transect, except at the scale of 96 to 105 m and 90 to 96 m for the potion of 150 to 210 m and 246 to 315 m of transect, respectively. There also is large variation at the end of the transect over a scale of 24 m or more. A few incidents of moderate variation (light blue) exist throughout the scale over the transect. A large variation (yellow) is present at the scale of 15 to 30 m in the area of 69 to 111 m, 165 to 190 m, and 270 m to the end of transect.

Figure 8 shows the cross wavelet spectrum between the elevation and the δ^{15}N value in the soil of the Davidson transect. The large covariances between the elevation and the δ^{15}N value exist at a scale of 54 m or more at the beginning and end of the transect and 96 m or more at the middle of the transect, whereas moderate covariances exist at the scale of 0 to 12 m and 24 to 54 m at the beginning of the transect and throughout the entire scale at the end of the transect. The covariances between δ^{15}N and the elevation at small scales are different from that at large scales, such as at 96 m or more over the entire transect and 24 m or more at the beginning of the transect and throughout the scale at the end of the transect. These areas are predominantly out of phase (left directed arrow). The relationship between δ^{15}N and elevation is indicated by the direction of the arrows. The left directed arrows at the scale of 24 to 42 m and 54 m or more at the beginning of the transect and 12 to 42 m at the end of the transect indicate the out of phase or the negative relationship between δ^{15}N and the elevation, which is also shown by general statistics. Since the statistically significant areas are less than 10 per cent of the total, these significant variations may be spurious. The remaining areas are not oriented to a single pattern and the relationship is quite complex at these scales and areas. With this complex phase relationship, it is very difficult to predict the relationship between δ^{15}N and the elevation. Generally, these variations are random at these scales. The covariance between δ^{15}N and elevation at the small scale is small compared to the covariance at the large scale; therefore, it is difficult to predict any relationship between δ^{15}N and elevation from the minor contribution of the variances at the smaller scale. The major covariances exist mainly at the large scales. Some covariances also exist at the two ends of transect, which are located at a higher elevation than the other points of the transect. Wavelet coherency analysis can establish whether or not these covariances can explain the location dependency.

Figure 9 shows the cross wavelet spectrum between the δ^{15}N of soil and the elevation of the Elstow transect. The larger covariances exist between the elevation and the δ^{15}N values at the section from 114 to 240 m of the transect at the scale of 30 to 48 m and at the scale of 96 m or more over the entire transect. The moderate covariances exist between δ^{15}N and the elevation from the scale of 12 to 24 m between section of 0 to 45 m of the transect, at the scale of 0 to 18 m at the end of the transect, and at the scale of 36 m or more at the section of 330 m to the end of the transect. These covariances are quite different from the covariances that exist at the scale of 30 to 48 m at the portion of 114 to 240 m of transect and at the scale of 96 m or more. These areas are predominantly out of phase (left directed arrow). This out of phase relationship indicates the negative correlation between δ^{15}N and the elevation. This relatively strong correlation is found in the depressions along the transect, which experiences frequent flooding. Identification of this correlation reveals the importance of considering scale and space in of sampling and analyses. Wavelet coherency analysis can give a better understanding of variability that otherwise might not be detected or explainable. Some other significant relationships exist only at the scale of 0 to 12 m at the beginning of the transect and at the scale of 0 to 18 m and 24 to 54 m at the end of the transect, but these areas are less than 10 per cent of the total, indicating that these significant variations may be spurious. In some places the arrows show in phase relationship too, indicating a positive relationship. The disoriented arrows (random) in

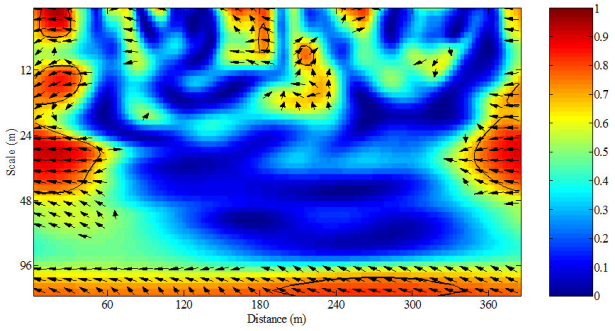

Fig. 10. Local wavelet coherency between the δ^{15}N in soil and the elevation of the Davidson transect. The horizontal axis shows the distance between sampling locations and the origin of transect. The vertical axis shows the scale. Arrows indicate the phase angles on wavelet spectra. Black solid line indicates the 90 per cent confidence level.

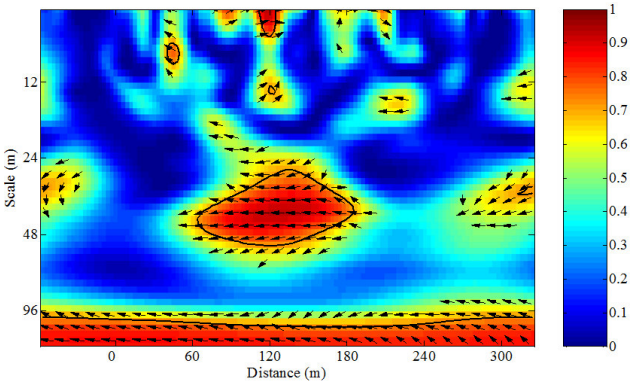

Fig. 11. Local wavelet coherency between δ^{15}N in soil and the elevation of the Elstow transect. The horizontal axis shows the distance between sampling locations and the origin of transect. The vertical axis shows the scale. Arrows indicate the phase angles on wavelet spectra. Black solid line indicates the 90 per cent confidence level.

the rest of the area at different scales indicate a complex relationship between the δ^{15}N in soil and the elevation. The small covariance at the small scale compared to the large covariance at the large scale contribute much less in predicting the relationship.

Figure 10 shows the wavelet coherency between δ^{15}N and elevation of the Davidson transect. Significant coherency between δ^{15}N and elevation exists at the scale of 0 to 6 m, 12 to 18 m, and 21 to 60 m at the beginning of the transect. The significant coherency also exists at 15 to 18 m and 21 to 45 m at the end of the transect. At these scales, the areas of significant variations are less than 10 per cent of the total, and these variations may be spurious. Also, large coherency exists at the scale of 96 m or more. Although the coherency at this scale is not completely statistically significant, the area covered is more than the area covered by the other small scales that are statistically significant. At this scale, the strong coherencies are mainly out of phase over the transect, suggesting a negative correlation. At the same time, the statistically significant coherency at the small scale also is out of phase, suggesting a negative correlation between δ^{15}N and elevation. The small scale coherency is mainly concentrated at the beginning and the end of the transect. Those sample points with low δ^{15}N are located at higher elevations than the other points of the transect. High δ^{15}N value exist over most of the transect except at the ends.

The Elstow transect (Fig. 11) shows a large significant coherency between δ^{15}N in soil and the elevation at two scales; 24 to 60 m over the section of 120 to 240 m and 96 m or more over the transect. These areas of significant variation are more than 10 per cent of the total and are indeed statistically significant. At these scales and locations, the coherency is predominantly out of phase, suggesting a negative relationship between δ^{15}N and the elevation. The Davidson transect could not give significant information about locations. At some of the small scales the coherency is weak and the phase relationship is random. Because the coherency is very little compared to the strong coherency at the scale of 24 to 60 m and 96 m or more, it does not affect the relationship showed by the large scale. The strong coherency at the high scales indicates the landscape scale relationship between δ^{15}N values and elevation.

These different levels of coherency between elevation and δ^{15}N are mainly due to landscape effects on water redistribution, which ultimately affects the biological activity in soil. In Saskatchewan semi arid environment, rain water runoff and snow drift are very common in upper knoll positions, leaving the area drier relative to lower slopes (Kachanoski and de Jong, 1988; Hayashi et al., 1998), likely favouring nitrification. Moreover, in these glacial till landscapes, the calcareous parent material often contributes to relatively high pH values on the knolls and thus ammonia volatilization may be favoured in these positions of the landscape. As a consequence, increased δ15N values in these positions may reflect the contribution of ammonia volatilization to the ^{15}N signature of the soil N. The water from precipitation and snowmelt concentrates mainly in the depression sections of the transect (Hayashi et al., 1998), triggering denitrification (Lemke et al., 1998; Davidson and Verchot, 2000). Denitrification, which favours the gaseous loss of the lighter ^{14}N isotope (Cheng et al., 1964; Ledgard et al., 1984; Sutherland et al., 1991; Kendall, 1998) likely contributed to the higher δ^{15}N values at the low topographic positions (Karamanos et al., 1981; Selles et al., 1986). At the small scale in other locations, the phase of the relationship is random, reflecting perhaps the competing soil processes of nitrification, denitrification and ammonia volatilization. There is strong coherency at the high scale over the entire transect. This transect has a number of small depressions in it that show very little change in the δ^{15}N values. Wavelet coherency shows that together the small depressions act as a large depression and therefore there is a high δ^{15}N value in the depressions

than at both ends. The coherency shown at both ends may be due to the position in the landscape. The knoll position is drier (i.e., aerobic), favouring either ammonia volatilization or nitrification processes, which could contribute to the high coherency at both ends of the transect.

Only when both variables at a scale make a large contribution to their total variances, will a high coherency between the two variables be meaningful (Si and Zeleke, 2005). For the Davidson transect, the large variances exist for both δ^{15}N and elevation at the large scale (60 m or more) over the entire transect. A moderate variance exists at the scale of 0 to 12 m, 12 to 21 m, and 24 to 48 m at the beginning and end of the transect. There are also high covariances at those scales and locations. Therefore, the high coherencies at those scales are physically meaningful. In the same way, the strong coherency at the scale of 24 to 60 m at 120 to 240 m distance and at the scale of 96 m or more over the transect for the Elstow transect is also physically meaningful.

Strong coherency exists at a few locations and at some scales. The strong coherency shows the relationships between δ^{15}N and elevation at the higher scale for both transects but not for all locations. The wavelet spectrum and the wavelet coherency of δ^{15}N and elevation help to identify the dominant landscape scale and the location of variation. Locally high coherency gives comprehensive information that will help us to identify and understand dominant soil processes. Wavelet coherency analysis is a powerful tool. The general statistics showed a relationship between δ^{15}N and the elevation for the Davidson transect, but failed to identify the relationship in the Elstow transect. Here the general statistics would give misleading information about the relationship, which would lead to a misidentification of soil processes, whereas the wavelet revealed the relationship clearly.

The Pearson correlation coefficient can only identify the linear relationship between two variables at the measurement scale (in this study, 3 m). The δ^{15}N values are the result of many interacting processes, and the dominant processes controlling δ^{15}N may change with landscape positions. It is clear from the Elstow transect that the phase changes, meaning negative and positive correlations coexist in the transect. The coexistence of positive and negative correlations could obscure correlations between elevation and δ^{15}N, leading to very low or non-significant Pearson correlation coefficients, which was found for the Elstow transect. However, in this case the wavelet coherency revealed a significant relationship between δ^{15}N values and elevation of the transect.

4 Conclusions

In this study, the relationship of δ^{15}N and elevation was analysed using wavelet spectra, cross wavelet, and wavelet coherency for the two transects. The wavelet spectra of the δ^{15}N values of Davidson transect shows some statistically significant small variations at small scale up to 12 m and some large variation at large scale, and elevation shows some large variation at large scale over most of the transect. The higher coherency at the beginning and at the end of the transect indicates a good correlation between δ^{15}N and elevation indicating the dominant location of variability over the landscape. Large variation of δ^{15}N and elevation at large scale makes a large contribution to the total variation which is revealed by high coherency at large scales indicating a dominant scale of variation over the landscape. The wavelet spectra of the δ^{15}N values of Elstow transect shows large variation at the scale of 48 m or more, located almost at the middle of the transect. This large variation of δ^{15}N, which shows a coherent relation with elevation at the depression section of the transect, indicates a location dependency of the landscape process. It suggests that frequent flooding within the depression (i.e., conditions favouring denitrification) has resulted in a location dependent relationship of δ^{15}N and elevation. The large coherency of δ^{15}N and elevation at the scale of 24 to 48 m at the middle of the transect indicates about the scale and location dependent landscape process. The cross wavelet and wavelet coherency are predominantly out of phase, showing the negative relationship between δ^{15}N and elevation for both transects. The higher coherency at both depression and knoll positions over the landscape indicates the occurrence of at least two N-cycling processes in the landscape which are mainly affected by the hydrology of the landscape as affected by elevation.

Acknowledgements. Funding for this project was provided by the Agricultural Development Fund (ADF) of Saskatchewan. Wavelet software was provided by C. Torrence and G. Compo, and is available at URL: http://paos.colorado.edu/research/wavelets/. Cross wavelet and wavelet coherence software were provided by A. Grinsted and is available at URL: http://www.pol.ac.uk/home/research/waveletcoherence/.

Edited by: Q. Cheng
Reviewed by: one anonymous referee

References

Bedard-Haughn, A., van Groenigen, J. W., and van Kessel, C.: Tracing 15N through landscapes: potential uses and precautions, J. Hydrol., 272, 175–190, 2003.

Blackmer, A. M. and Bremner, J. M.: Inhibitory effect of nitrate on reduction of N_2O to N_2 by soil microorganisms, Soil Biol. Biochem., 10, 187–191, 1978.

Bremer, E. and van Kessel, C.: Appraisal of nitrogen-15 natural-abundance method for quantifying dinitrogen fixation, Soil Sci. Soc. Am. J., 54, 404–411, 1990.

Bremner, J. M. and Tabatabai, M. A.: ^{15}N enrichment of soils and soil derived nitrate, J. Environ. Qual., 2, 363–365, 1973.

Broadbent, F. E., Rauschkolb, R. S., Lewis, K. A., and Chang, G. Y.: Spatial variability of nitrogen-15 and total nitrogen in some virgin and cultivated soils, Soil Sci. Soc. Am. J., 44, 524–527, 1980.

Bryan, B. A., Shearer, G.B., Skeeters, J. L., and Kohl, D. H.: Variable expression of the nitrogen isotope effect associated with denitrification of nitrite, J. Biological Chem., 258, 8613–8617, 1983.

Cheng, H. H., Bremner, J. M., and Edwards, A. P.: Variations of ^{15}N abundance in soils, Science, 146, 1574–1575, 1964.

Davidson, E. A. and Verchot, L. V.: Testing the hole in the pipe model of nitric oxide emissions from soils using the TANGENT database, Global Biogeochem. Cy., 14, 1035–1043, 2000.

Elliott, J. A. and de Jong, E.: Quantifying denitrification on a field scale in hummocky terrain, Can. J. Soil Sci., 72, 21–29, 1992.

Farge, M.: Wavelet transform and their applications to turbulence, Annu. Rev. Fluid Mech., 24, 395–457, 1992.

Graps, A.: An introduction to Wavelets, IEEE Comput. Sci. Eng., 2, 1–18, 1995.

Grinsted, A. J. C., Moore, S., and Jevrejeva, S.: Application of cross wavelet transform and wavelet coherence to geophysical time series, Nonlinear Processes. Geophys., 11, 561–566, 2004.

Hayashi, M., van der Kamp, G. and Rudolph. D.L.: Water and solute transfer between a prairie wetland and adjacent uplands, 1. Water balance, J. Hydrol. 207, 42–55, 1998.

He,Y., Guo, X., and Si, B. C.: Detecting grassland spatial variability by a wavelet approach, Int. J. Remote Sens., 28, 1527–1545, 2007.

Heaton, T. H. E.: Isotopic studies of nitrogen pollution in the hydrosphere and atmosphere: A review, Chem. Geol., 59, 87–102, 1986.

Herbal, M. J. and Spalding, R. F.: Vadose zone fertilizer-derived nitrate and δ^{15}N extracts, Ground Water, 31, 376–382, 1993.

Höberg, P.: 15N natural abundance in soil-plant systems, New Phytol., 137, 179–203, 1997.

Jenkinson, D. S. and Parry, L. C.: The nitrogen cycle in the Broadbalk wheat experiment: A model for the turnover of nitrogen through the soil microbial biomass, Soil Biol. Biochem., 21, 535–541, 1989.

Johannisson, C. and Höberg, P.: 15N abundance of soils and plants along an experimentally induced forest nitrogen supply gradient, Oceologia, 97, 322–325, 1994.

Kachanoski, R. G. and de Jong. E.: Scale dependence and the temporal persistence of spatial patterns of soil water storage, Water Resour. Res., 24, 85–91, 1988.

Karamanos, R. E., Voroney, R. P., and Rennie, D. A.: Variations in natural N-15 abundance of Central Saskatchewan soils, Soil Sci. Soc. Am. J., 45, 826–828, 1981.

Keeny, D. R.: Nitrogen availability indices, Methods in Soil Analysis, Part 2, A. L. Page (Eds.), 2nd Eds. Agron. Monogr., 9, ASA and SSSA, Madison, WI. 13, 711–734, 1982.

Kendall, C.: Tracing nitrogen sources and cycling in catchments, in: Isotope tracers in catchment hydrology, edited by: Kendall, C. and McDonnell, J. J., Elsevier, NY, 519–576, 1998.

Korom, S. F.: Natural denitrification in the saturated zone: A review, Water Resour. Res., 28, 1657–1668, 1992.

Kreitler, C. W.: Determining the source of nitrate in ground water by nitrogen isotope studies, Rept. Of Invest, 83, Univ. Of Texas at Austin, TX, Bureau of Econ. Geol., 53, 1975.

Kumar, P. and Foufoula Georgiou, E.: Wavelet analysis of geophysical applications, Rev. Geophys., 35, 385–412, 1997.

Kumar, P. and Foufoula-Georgiou, E.: A multicomponent decomposition of spatial rainfall fields: 1. Segregation of large- and small-scale features using wavelet transforms, Water Resour. Res., 29, 2515–2532, 1993.

Labat, D., Ababou, R., and Mangin, A.: Rainfall runoff relations forkarstic springs, Part II: Continuous wavelet and discrete orthogonal multi-resolution analysis, J. Hydrol., 238, 149–178, 2000.

Lark, R. M. and Webster, R.: Analysis and elucidation of soil variation using wavelets, Eur. J. Soil Sci., 50, 185–208, 1999.

Lark, R. M. and Webster, R.: Changes in variance and correlation of soil properties with scale and location: Analysis using an adapted maximal overlap discrete wavelet transform, Eur. J. Soil Sci., 52, 547–562, 2001.

Ledgard, S. F., Freney, J. R., and Simpson, J. R.: Variations in natural enrichment of ^{15}N in the profiles of some pasture soils, Aust. J. Soil Res., 22, 155–164, 1984.

Lemke, R. L., Izaurralde, R. C., and Rothrock, D. A.: The discrete wavelet transform and the scale analysis of the surface properties of sea ice, IEEE T. Geosci. Remote, 34, 771–787, 1998.

Mallat, J.: A wavelet tour of signal processing, Academic Press, New York, 1–11, 1999.

Maraun D. and Kurths, J.: Cross wavelet analysis: Significance testing and pitfalls, Nonlin. Processes. Geophys., 11, 505–514, 2004.

Mariotti, A., Germon, J. C., Hubert, P., Kaiser, P., Letolle, R., Tardieux, A., and Tardieux, P.: Experimental determinations of nitrogen kinetics isotope fractionation: Some principles: Illustration for the denitrification and nitrification processes, Plant Soil, 62, 413–430, 1981.

Meyer, S., Kelley, B., and O'Brien, J.: An introduction to wavelet analysis in oceanography and meteorology: with application to the dispersion of Yanai waves, Mon. Weather Rev., 121, 2855–2866, 1993.

Moulin, A. P., Anderson, D. W., and Mellinger, M.: Spatial variability of wheat yield, soil properties and erosion in hummocky terrain, Can. J. Soil Sci., 74, 219–228, 1994.

Natural Resources Canada:http://gocanada.about.com/od/canadatravelplanner/ig/Canada-Maps.--0v/Saskatchewan-Map.htm, 2001.

Nielsen, D. R. and Wendorth, O.: Spatial and temporal statistics: sampling field soil and their vegetation, Catena Verlag, Reiskirchen, Germany, 2003.

Pardo-Iguzquiza E. and Rodriguez-Tovar, F. J.: The permutation test as a non-parametric method for testing the statistical significance of power spectrum estimation in cyclostratigraphic research. Earth Planet. Sc. Lett., 181, 175–189, 2000.

Pennock, D. J., Anderson, D. W., and de Jong, E.: Landscape scale changes in indicators of soil quality due to cultivation in Saskatchewan, Canada, Geoderma, 64, 1–19, 1994.

Riga, A., van Praag, H. J., and Brigode, N.: Natural abundance of nitrogen isotopes in certain Belgium forest and agricultural soils under certain cultural treatments, Geoderma, 6, 213–222, 1970.

Robinson: δ15N as an integrator of the nitrogen cycle, Trends Ecol. Evolut., 16, 153–162, 2001

Selles, F., Karamanos, R. E., and Kachanoski, R. G.: The spatial variability of nitrogen-15 and its relation to the variability of other soil properties, Soil Sci. Soc. Am. J., 50, 105–110, 1986.

Shearer, G. and Kohl, D. H.: N_2 fixation in field settings: Estimates based on natural ^{15}N abundance, Aust. J. Plant Physiol., 13, 699–756, 1986.

Shearer, G., Kohl, D. H., and Chien, S. H.: The nitrogen-15 abundance in a wide variety of soils, Soil Sci. Soc. Am. J., 42, 899–902, 1978.

Si, B. C. and Farrell, R. E.: Scale dependent relationships between wheat yield and topographic indices: A wavelet approach, Soil Sci. Soc. Am. J., 68, 577–588, 2004.

Si, B. C. and Zeleke, T. B.: Wavelet coherency analysis to relate saturated hydraulic properties to soil physical properties, Water Resour. Res., 41, W11424, doi:10.1029/2005WR004118, 2005.

Si, B. C.: Spatial and scale dependent soil hydrolic properties: a wavelet approach, Pachepsky, Y., Radcliffe, D. E., and Selim, H. M. (Eds.), Scaling method in soil physics, CRC Press, New York, 163–178, 2003.

Si, B. C.: Spatial scaling analyses of soil physical property: A review of spectral and wavelet methods. Vadose Zone J., accepted, 2007.

Smith, M. S. and Tiedje, J. M.: Phases of denitrification following oxygen depletion in soil, Soil Biol. Biochem., 11, 261–267, 1979.

Sorenson, J., Tiedje, J. M., and Firestone, R. B.: Inhibition by sulphide of nitric and nitrous oxide reduction by *Pseudomonas fluorescens*, Appl. Environ. Microb., 39, 105–108, 1980.

Sutherland, R. A., van Kessel, C., and Pennock, D. J.: Spatial variability of nitrogen-15 natural abundance, Soil Sci. Soc. Am. J., 55, 1339–1347, 1991.

Sutherland, R. A., van Kessel, C., Farrell, R. E. and Pennock, D. J.: Landscape scale variations in plant and soil nitrogen-15 natural abundance, Soil Sci. Soc. Am. J., 57, 169–178, 1993.

Torrence, C. and Compo, G. P.: A practical guide to wavelet analysis, Bull. Am. Meteorol. Soc., 79, 61–78, 1998.

Torrence, C. and Webster, P. J.: Interdecadal changes in the ENSO-monsoon system, J. Climate, 12, 2679–2690, 1999.

Townsend, M. A.: Use of natural nitrogen-15 isotope method to identify sources of nitrate in ground water near Oberlin, Kansas, Kansas Geological Survey, Open file report, 50, 20, 2001.

Venterea, R. T., Lovett, G. M., Groffman, P. M., and Schwarz, P. A.: Landscape patterns of net nitrification in a Northern Hardwood conifer forest, Soil Sci. Soc. Am. J., 67, 527–539, 2003.

Yates, T. T., Si, B. C., Farrell, R. E., and Pennock, D. J.: Wavelet spectra of nitrous oxide emission from hummocky terrain during spring snowmelt, Soil Sci. Soc. Am. J., 70, 1110–1120, 2006.

Yoshida, N., Morimoto, H., Harane, M., Koike, I., Matsuo, S., Wada, E., Saino, T., and Hattori, A.: Nitrification rates and ^{15}N abundances of N_20 and NO_3^- in the western North Pacific. Nature, 342, 895–897, 1989.

Zebarth, B. J. and de Jong, E.: Water flow in a hummocky landscape in Central Saskatchewan, Canada: I. Distribution of water and soil, J. Hydrol., 107, 309–327, 1989.